An MXene-doped PVA/PVP hydrogel-based strain sensor applicable in liquid environment

Ying Yi[1,2] ⓘ, Mu Chiao[3] ⓘ, Khaled A Mahmoud[4] ⓘ and Bo Wang[2,*] ⓘ

[1] School of Mechanical Engineering and Electronic Information, China University of Geosciences, Wuhan, People's Republic of China
[2] Division of Information and Computing Technology, College of Science and Engineering, Hamad Bin Khalifa University, Doha, Qatar
[3] Department of Mechanical Engineering, University of British Columbia, Vancouver, BC, Canada
[4] Qatar Environment and Energy Research Institute (QEERI), Hamad Bin Khalifa University, Doha, Qatar

E-mail: bwang@hbku.edu.qa

CrossMark

Abstract

Hydrogel-based strain sensors garner immense interest in view of their excellent mechanical properties and sensing performance for applications in a liquid environment. However, swelling of hydrogel in liquid would significantly degrade its electro-mechanical performance. This work presents a new fabrication method for an anti-swellable hydrogel synthesized by mixing titanium carbide ($Ti_3C_2T_x$) MXene nanoparticles with polyvinyl alcohol (PVA) and polyvinylpyrrolidone (PVP) blend. A strong interaction can be formed between the double-network PVA/PVP hydrogel matrixes through a cyclic freezing–thawing method, and the addition of the MXene further improves the electro-mechanical properties of the hydrogel. Our results reveal that the synthesized MXene-PVA/PVP hydrogel (MX-hydrogel) improves the gauge factor of the sensor by 61% compared to that of a hydrogel without adding MXene nanoparticles when applied as a strain sensor. Moreover, the MX-hydrogel formed in its recovery stage exhibits a volume-limited swelling, which can be regarded as anti-swellable behavior. Finally, the synthesized MX-hydrogel's structural, elastic, thermal, and electrical properties are investigated, paving the way toward dosage monitoring as a demonstration of the application.

Keywords: MXene, PVA/PVP hydrogel, anti-swellable property, strain sensor

(Some figures may appear in colour only in the online journal)

1. Introduction

Recently, flexible electronics have drawn tremendous interest, exemplified by enormous applications such as human–computer interactions [1], intelligent monitoring [2, 3], proprioceptive sensor [4], etc. The substrates that endow these electronics with stretchability and deformability are typically fabricated by the elastomers such as rubber fiber [4], polydimethylsiloxane (PDMS) [5], polyurethane [6], polyetherimide [7], Ecoflex [8], etc. Compared to elastomers, hydrogels are verified as a more suitable candidate for flexible and wearable electronics owing to their better mechanical properties, tissue-like moduli, and biocompatibility [9]. Furthermore, hydrogels have three-dimensional (3D) cross-linked structures and hydrophilic groups on polymers, combining the advantages of both liquid and solid together, demonstrating more widespread application potential in sensors [10],

---

* Author to whom any correspondence should be addressed.

tissue engineering [11], and interference shields [12]. However, hydrogels are usually swellable behavior in water, limiting their applications such as marine exploration [13], underwater sensing [14], or deployment in humid environments. Furthermore, swelling of the hydrogel suppresses its mechanical strength and reduces its conductivity because of the percolation-diluted conductive network [15], thus degrading its sensitivity when used as sensor substrates. Several strategies were introduced to develop non-swelling hydrogels, thus allowing stable sensing in wet environments, including coordination interactions, hydrophobic aggregation, and encapsulation technology [16–18]. However, these approaches may reduce their high stretchability, desirable modulus, or signal stability [13]. Therefore, it is imperative to explore a simple method to fabricate an anti-swellable hydrogel without reducing its electro-mechanical performance.

Besides the substrate, the sensing materials also play a critical role in hydrogel-based sensors [19]. Nanomaterials, such as metal nanoparticles, carbon nanotubes (CNTs), and graphene, are synergetic ingredients widely used to fabricate conductive nanocomposite hydrogels. The addition of nano-scale particles to the polymer can enhance its mechanical, electrical, and optical performance. For example, adding titanium dioxide nanoparticles to polyvinyl alcohol (PVA)/chitosan (CN)–lithium (Li) polymer can increase both the electrical conductivity and mechanical performance [20]. Cai *et al* used single-walled CNTs composited PVA hydrogel to serve as a piezoresistive strain sensor, which can withstand ten times elastic deformation and exhibit fast electrical healing ability. However, it is challenging to uniformly disperse these nanomaterials into the hydrophilic hydrogel because of their hydrophobic nature [21].

As an emerging two-dimension (2D) material, the family of transition metal carbide (MXenes) exhibits great potential as a sensing material due to their excellent hydrophilicity, high electrical conductivity, large interlayer space, rich surface chemistry, and tunable electronic structure [22–25]. Moreover, MXene nanoparticles can not only be uniformly distributed in hydrogels without aggregation thus forming stable conductive pathways, but also can build hydrogen bonds with polymer chains via the multi-physical interactions to improve the mechanical performance of the MXene-hydrogel composite [26]. Note that MXene belongs to the chemical family $M_{n+1}X_nT_x$, where M means a transition metal, X denotes C and/or N, T_x represents surface functional groups, and $n = 1, 2$, or 3 [27]. Under a tension or compression condition, the sliding and stacking of MXene nanoparticles effectively change the conductive paths, thereby resulting in resistance variations [28, 29]. With such a piezoresistivity, the composite, by incorporating MXene into the hydrogel can serve as an excellent strain or pressure sensor [30].

This paper adopts PVA and polyvinylpyrrolidone (PVP) as the hydrogel substrate. PVA is a biocompatible, water-soluble, and non-toxic polymer which can be fabricated for deformable films. However, it must integrate the other polymer for higher stretchability in practical applications [31]. PVP, a polymeric additive with high hydrophilicity and biocompatibility, is usually mixed with the PVA to form a strong hydrogen bonding between the hydroxyl (–OH) and carbonyl (C=O) groups of PVA and PVP in their blend solution [32, 33]. The PVA/PVP polymer blend exhibits an improved mechanical performance compared to PVA alone [34], making it popular for fabricating lightweight, ultra-elastic composite hydrogel. With the addition of the MXene nanoparticles, a double-network MXene-PVA/PVP hydrogel (MX-hydrogel) can be formed via a one-step freezing–thawing synthesis process [35, 36]. Unlike the previously reported hydrogels showing continuous swelling behaviors in liquid, we observe that naturally evaporating the MX-hydrogel and then soaking the dried one in water would recover the hydrogel which has a swelling stop, thus such a recovered hydrogel can be regarded as an anti-swellable type. As verified experimentally, the developed MX-hydrogel exhibits excellent mechanical properties such as stretchability, puncture resistance, and stability. As a demonstration of application, an electrochemically actuated drug delivery device using the MX-hydrogel-based strain sensor for dosage monitoring was presented. Such an anti-swellable MX-hydrogel strain sensor has a high potential for applications such as implantable electronics, artificial skin, in-liquid sensing, etc.

2. MXene-doped PVA/PVP hydrogel (MX-hydrogel)

2.1. MX-hydrogel preparation

The preparation of the MXene solution involves two steps, including the selective etching from MAX phases ($M_{n+1}AX_n$) and the delamination of MXenes [25]. In this work, 250 mg of Ti_3AlC_2 (MAX phase, purchased from Y-Carbon, Ltd) was added gradually to a Teflon tube containing 5 ml of LiF (400 mg)/Hydrochloric acid (HCl) acid solution, which undergoes continuous stirring for 24 h at room temperature. The residue acidic black suspension containing etched multi-layered (ML) $Ti_3C_2T_x$ was then washed repeatedly with deionized (DI) water until the pH of the supernatant is above 6. The residual ML $Ti_3C_2T_x$ was then collected by centrifugation. The delamination was carried out by bath sonication of the colloidal solution in degassed water for 40 min to obtain the desired single or few-layered $Ti_3C_2T_x$ from the supernatant. A flaky powder was obtained by freeze-drying and was used in the flowing steps [37].

PVA/PVP polymer blend was prepared following an optimized mixture ratio as reported in [30]. First, 1.8 g of PVA powder (Mw ∼94 k, Sigma-Aldrich Co.) was mixed with 11.4 ml of DI water at 90 °C. The PVA solution became transparent after at least 1 h of constant stirring, indicating that the powder was fully dissolved. Next, the same stirring was performed to dissolve 0.3 g of PVP powder (Mw ∼40 k, Sigma-Aldrich Co.) in 1.5 ml of DI water. Meanwhile, 0.5 ml of sulphuric acid was slowly added into the above-prepared PVA and PVP solutions which were then stirred; with the catalysis of sulfuric acid, the polymer chains of PVA and PVP (PVA–OH and PVP–C=O) self-assembled into the 1,3-dioxane polymer [38]. Then, about 1.5 ml of the delaminated MXene solution (∼0.01 mg ml^{-1}) was added to the PVA/PVP solution following the same stirring operation to obtain a uniform dispersion
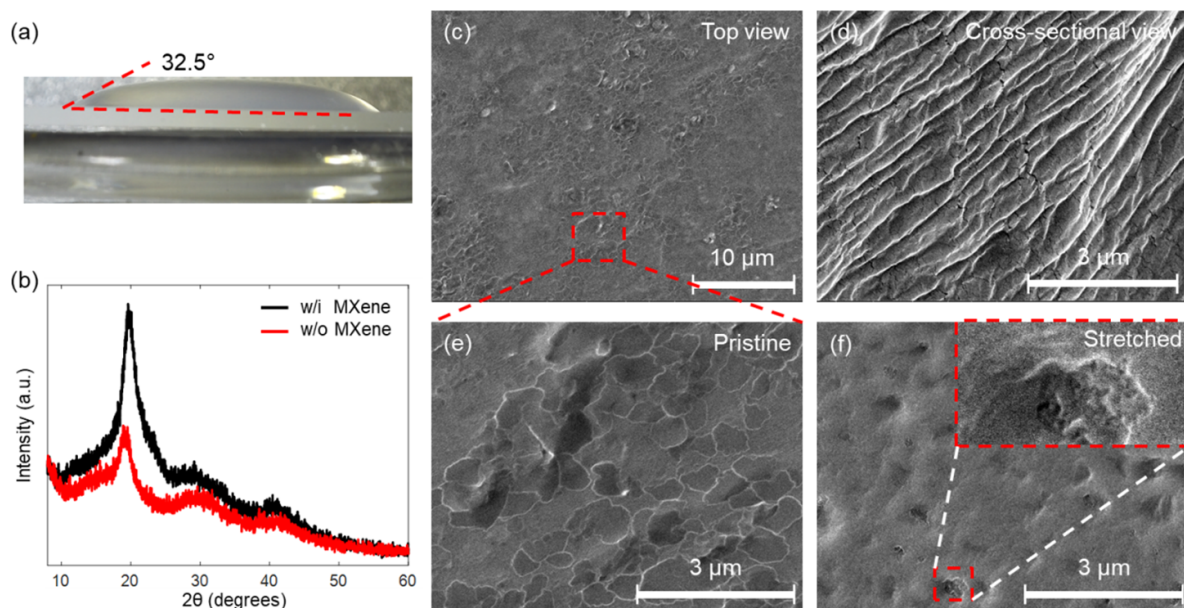
Figure 1. (a) Hydrophilicity analysis of PVA/PVP polymer blend; (b) XRD patterns of PVA/PVP hydrogel with and without MXene; SEM images of the MXene from (c) top view; (d) cross-sectional view; (e) magnification view of the pristine state; (f) particle distribution under external stretching.

of the MXene nanoparticles in the viscous PVA/PVP solution. Different contents of the MXene in the hydrogel would induce different electro-mechanical performances [30], however, this kind of work is out of research interest of this paper as it may greatly increase the lengthy without bringing new observation on the anti-swelling behavior of the hydrogel. Finally, the MX-hydrogel film was formed by repeatedly freezing ($-20\,^{\circ}$C for at least 12 h) and thawing (room temperature for at least 4 h) the MXene-doped PVA/PVP polymer blend. The freezing and thawing operations were repeated three times to form a robust MX-hydrogel film because the freezing and thawing approach can change the randomly curled PVA chains into locally ordered nano-crystalline domains and form crystal segments.

2.2. Structural properties of the synthesized MX-hydrogel

Contact angle measurement was widely used to evaluate hydrophilicity. As shown in figure 1(a); the PVA/PVP polymer blend has a contact angle of 32.5°, which confirms that the blend is hydrophilic. Figure 1(b) shows the x-ray diffraction (XRD) spectra of the PVA/PVP hydrogel with and without MXene at room temperature. The intensity of the PVA/PVP hydrogel peaks at 19.6°, which is related to the semi-crystalline nature of the PVA. This result agrees with an earlier study on PVA/PVP hydrogel [39]. With the addition of the MXene nanoparticles, the intensity peak decreases because the crystallinity of the PVA/PVP hydrogel has been destroyed [40].

Scanning electron microscope (SEM) of the MX-hydrogel film was studied to verify its surface morphologies and to check the distribution of MXene nanoparticle distribution in the PVA/PVP blend under relaxed and stretched states. Typically, pristine PVA/PVP hydrogel has a smooth and homogeneous surface [39]; however, with the addition of the MXene, the dispersion of nano-scale MXene modified the surface morphology of the hydrogel film, as shown in figure 1(c). The cross-sectional view of the multiple-layer structure of the MX-hydrogel is shown in figure 1(d). It confirms that the MXene nanoparticles distribute homogeneously over the entire surface of the PVA/PVP blend. With the magnification, as shown in figure 1(e), nano-scale structures of the MXene differ somewhat in size, but all of them are linked to each other without aggregations.

The varying 3D network structure of the MXene nanoparticles embedded within the hydrogel matrix is the main reason causing the resistance change under tensile deformation in MX-hydrogel. Specifically, when the MX-hydrogel is stretched, the gap between the MXene nanoparticles increases, prolonging effective conductive paths and reducing the chance of contact with the hydrogel matrix. As SEM characterization has demonstrated, as shown in figure 1(f), the space between the MXene nanoparticles is significantly enlarged, and the particles protruded due to the geometrical changes of the hydrogel matrix caused by the stretching. As a result, the resistance of the MX-hydrogel increases in response to external stretching and vice versa.

2.3. Electromechanical properties of the synthesized MX-hydrogel

The synthesized MX-hydrogel film was manually stretched, curled, folded, poked, and loaded to demonstrate its flexibility and mechanical robustness, as illustrated in figures 2(a)–(e). Even under large deformation, the MX-hydrogel can always restore to its original state once the external forces are removed showing excellent resilience. Particularly, the MX-hydrogel can undergo a certain level of puncture force. As illustrated in
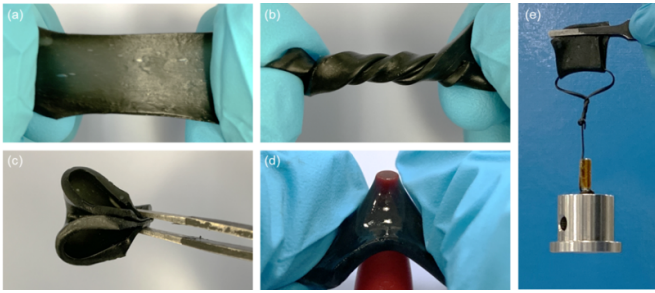
Figure 2. A freestanding MXene doped PVA/PVP hydrogel film being (a) stretched; (b) twisted; (c) folded; (d) poked; (e) loaded.

figure 2(d), the center of the hydrogel is not punctured under the localized stress concentration imposed by the plastic cone, which implies that the hydrogel film is elastic to withstand inhomogeneous deformations. A load of 100 g was applied to the folded sample to verify the MX-hydrogel film's toughness. As depicted in figure 2(e), breakage or crack was not observed within the testing time.

Apparent shrinkage in the size of the MX-hydrogel was found if the sample was placed in the air, because the water molecules naturally evaporate from the MX-hydrogel. Continuous loss of water molecules turns the MX-hydrogel into a dried and stiff state. However, for our synthesized MX-hydrogel, soaking the dried sample in water can recover it to a moist form as water molecules are adsorbed on vacancies and hydrophilic groups via hydrogen bonds [25]. As shown in figure 3(a), the original thickness of a tested MX-hydrogel sample was 0.6 mm. However, it decreased to 0.15 mm after water evaporation. Soaking the sample in water can restore its thickness to 0.4 mm at its maximum (regarded as a 'swelling stop'). It indicates that the developed MX-hydrogel is not continuously swellable after the drying and soaking process because the inner structure and volume of the PVA/PVP hydrogel have been permanently changed after it is dried.

First, the developed MX-hydrogel (at its initial state) was immersed in the water bath of a dynamic mechanical analyzer (DMA Q8000, PerkinElmer Inc., Waltham, MA, USA) to avoid a negative influence on the mechanical performance caused by the water evaporation in the air. The tensile test was repeated three times, and the hydrogel's stress–strain curves were measured, as depicted in figure 3(b), and no crack or breaking on the hydrogel surface was found. The MX-hydrogel dried and lost its elasticity after about 24 h if it was not placed in a sealed container. In this work, the above-tested MX-hydrogel sample was naturally dried and then soaked in water for recovery. The same tensile tests were repeated for the recovered MX-hydrogel in liquid. The stress–strain curves of the soaked sample are shown in figure 3(c). Comparing figures 3(b) and (c), Young's modulus of the MX-hydrogel increases for the soaked sample, with the induced elasticity reduction being irreversible due to the structural damage [41].

To further investigate the mechanical properties of the initial MX-hydrogel and its recovered state, the DMA was used to measure the stress–strain curves of the MX-hydrogel film at its different states. The MX-hydrogel was naturally thawed

in the air after being taken out from the fridge (-20 °C). Testing was performed at the 5th, 6th, and 7th hours of the thawing stage. If the thawing time is too short (e.g. less than 5 h in this work), the MX-hydrogel is too fragile to withstand any tension or pressure. With an increased thawing time, the tensile stress of the MX-hydrogel increased accordingly, as shown in figure 3(d). It is reasonable that the mechanical elasticity of the MX-hydrogel degrades with a continuous loss of water molecules.

Next, the conductivity of the MX-hydrogel was evaluated in air and liquid. A digital multimeter (Keithley 2110, Tektronix, Beaverton, OR, USA) was used to record the resistance of the sample. Figure 3(e) shows the MX-hydrogel resistance without any strain when placed in liquid. A stable resistance of 2.128 KΩ $\pm 0.81\%$ can be observed. In contrast, the resistance of the same sample placed in the air increased significantly with time because of the continuous loss of water [10]. This verified that our synthesized MX-hydrogel is an excellent material applicable in the aqueous environment (e.g. underwater, body surface, etc). For most nano-materials, temperature plays a critical role and could affect the material's performance. In our testing, the MX-hydrogel sample was immersed in a water bath, and its resistances at different liquid temperatures (20 °C–40 °C) were recorded. As shown in figure 3(f), its resistance drops about 0.6 KΩ for every 10 °C of temperature increase. This result agrees with the thermo-conductive property of the PVA hydrogel. Moreover, it was observed that the MX-hydrogel has a temperature tolerance of about 42 °C, the MX-hydrogel could dissolve when placed above this temperature.

2.4. MX-hydrogel-based strain sensor

The gauge factor (GF), defined as GF $= (\Delta R/R)/\varepsilon$, is often used to characterize the piezoresistivity of a strain sensor, where $\Delta R/R$ refers to the resistance change ratio under an applied strain ε. Herein, ΔR can be calculated by $\Delta R = R_\mathrm{r} - R$, with R_r and R being the sensor resistance with and without strain, respectively. Figure 4(a) shows that the MX-hydrogel sample can stretch to a strain of 20%, and no breakage and crack on the surface were observed during the stretching, implying that such a strain was within a safe range. The MX-hydrogel was stretched and released repeatedly; its $\Delta R/R$ was recorded, as shown in figure 4(b). Maximum strain in each cycle increased from 5% to 20% with an increasing step of 5%, and the $\Delta R/R$ increased with the strain increase over consecutive time and dropped corresponding to the release, suggesting an excellent tracking ability for the stretching and releasing processes.

Finally, the $\Delta R/R_\mathrm{s}$ of the hydrogels with and without adding MXene were compared. As shown in figure 4(c), different from the PVA/PVP hydrogel reported in [30], in which almost no resistance change response to strain for the range up to 40% [30], our PVA/PVP hydrogel exhibits a significant sensing performance because of the fabrication step of adding sulphuric acid as a catalyzer. The results indicate that the $\Delta R/R$ increases to 27% with the applied strain increasing to 36%, giving an average GF of 0.75. When the MXene is incorporated, the
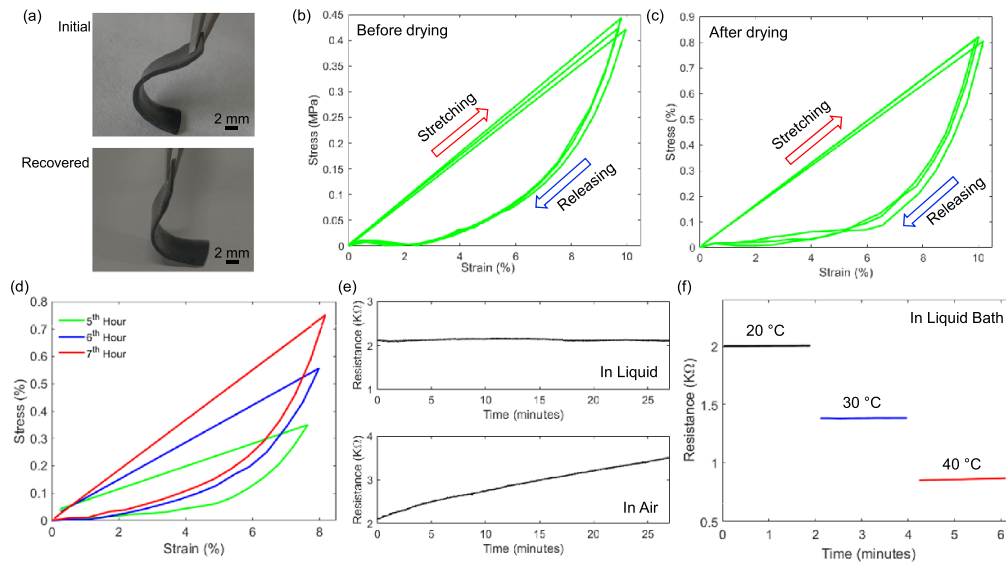
Figure 3. (a) Size change of the MX-hydrogel under its initial and recovered states; (b) stress–strain curves of the MX-hydrogel in air at different thawing time; (c) and (d) stress–strain curves of the MX-hydrogel before and after drying (water evaporation); (e) resistance of the MX-hydrogel in ambient and in liquid; (f) resistance of the recovered MX-hydrogel at different temperatures in liquid.
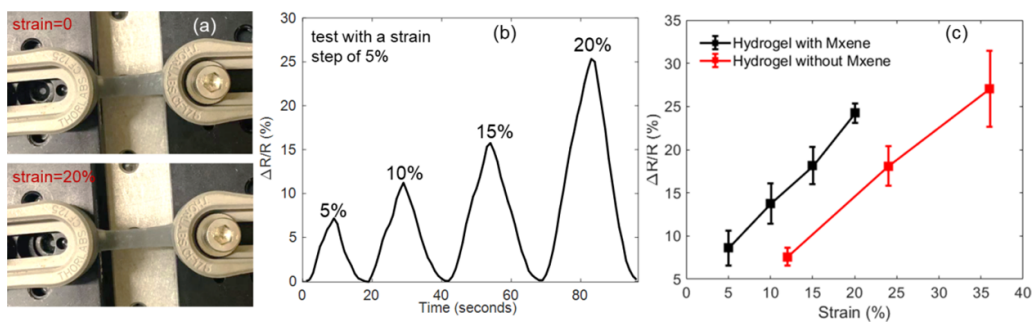

Figure 4. The electromechanical performances of the hydrogel-based strain sensor. (a) Illustration of prolongation of the MXene composited hydrogel sample under a maximum strain of 20%; (b) $\Delta R/R$ under cyclic stretching−releasing at strains of 5, 10, 15 and 20%, respectively; (c) $\Delta R/R$ comparison between the hydrogel with and without adding MXene.

$\Delta R/R$ violently increases with an increasing strain, as can be observed that an average $\Delta R/R$ of 24.2% is achieved at a strain of 20%, indicating a GF of about 1.21. Therefore, adding MXene to the pristine PVA/PVP hydrogel increases the GF by 61%, which is a great advantage for using the MX-hydrogel for strain sensing.

As mentioned above, the inner structure of the MX-hydrogel changes after it becomes dried; accordingly, its piezoresistivity change is worth exploring before and after suffering from natural drying, although soaking the dried hydrogel can partially restore its elasticity. To investigate the piezoresistive sensitivity of the newly fabricated MX-hydrogel before and after drying and soaking, the corresponding $\Delta R/R_s$ were recorded under cyclic loading and releasing operations. The MX-hydrogel sample was immersed in the DMA's water bath during testing. As shown in figure 5, for the newly fabricated sample, with a strain of 8%, a $\Delta R/R$ of $10.55 \pm 0.53\%$ can be achieved, corresponding to a GF of about 1.32. A similar test was performed for the same sample which underwent drying and soaking, and although a GF reduction of 42% is found, it is still much better than prior arts [42].

3. Application of the synthesized MX-hydrogel for dosage monitoring

As a real demonstration of application in liquid, the MX-hydrogel-based strain sensor was used for dosage monitoring in an electrolytic drug delivery device. Unlike the PDMS actuating membrane used for drug delivery [43–45], the PVA/PVP hydrogel film has excellent gas non-permeability, which can avoid the risk of bubble leakage during drug delivery. Figure 6(a) shows a cross-sectional view of the electrolytic actuator assembling with a thin MX-hydrogel diaphragm (thickness: 50 μm). The electrolysis electrode was fabricated following standard photolithography and sputtering processes on a silicon wafer, it had an interdigitated shape of titanium/platinum (Ti/Pt) deposition layers, and the detailed fabrication procedure and structure of the electrolytic actuator were reported in [46]. A DC power source was used to activate the electrolytic reaction inside the electrolytic chamber. As a result, the DI water that acts as an electrolyte was electrolyzed into H_2 and O_2. Consequently, the electrolysis bubble deforms the MX-hydrogel diaphragm, as shown in figure 6(b), the
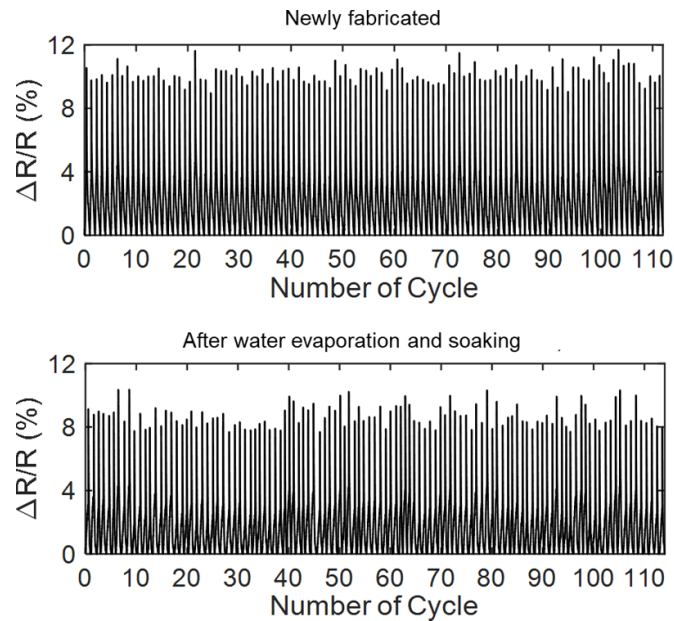
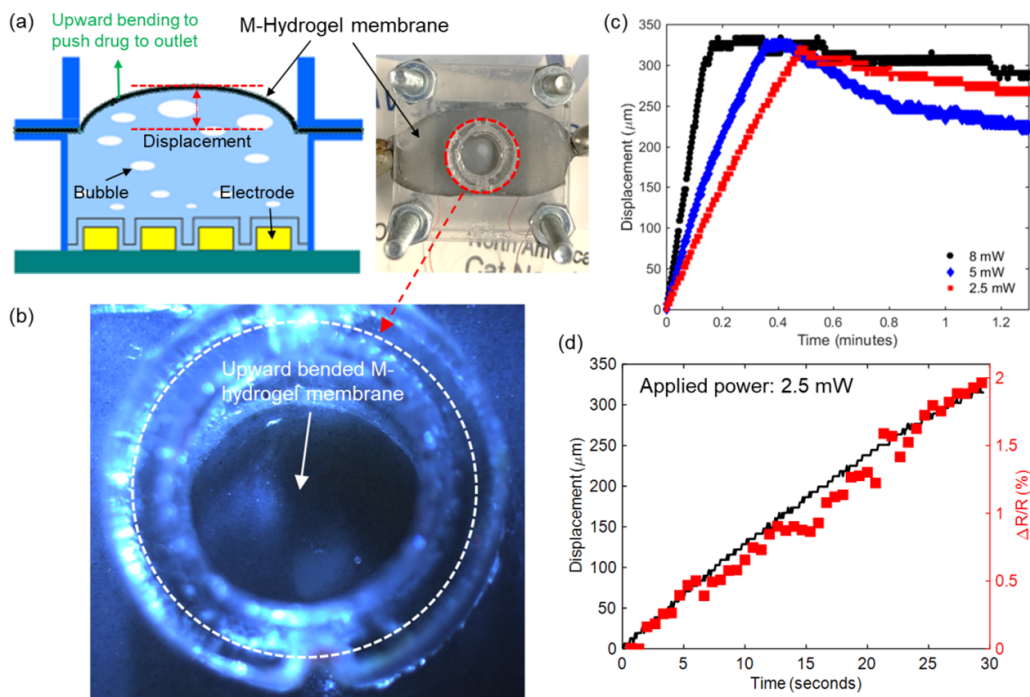**Figure 5.** Comparisons of the MX-hydrogel before and after the drying.

Figure 6. (a) Prototype of drug delivery device using Mxene composited hydrogel membrane as dosage sensor; (b) Magnification view of the deformed membrane upon electrolysis-bubble generation; (c) Membrane displacement with different applied power; (d) Correlation between the $\Delta R/R$ and membrane displacement.

deformed area of the MX-hydrogel diaphragm (highlighted by a red ring) functions as a dosage sensor. The membrane displacement, defined as the maximum vertical distance between its baseline and deflection, can indicate the volume of the drug delivered [44]. A laser Doppler vibrometer (OFV-5000, Polytec Inc., Irvine, CA, USA) was used to measure the displacement under different actuation power, with the MX-hydrogel diaphragm resistance being recorded.

As shown in figure 6(c), it took 31, 20, and 14 s to achieve a membrane displacement of about 322 μm using an actuation power of 2.5 mW, 5 mW, and 8 mW, respectively. Apparently, the higher power is applied, the faster the MX-hydrogel membrane deforms due to faster electrolysis bubble generation. The volume of the drug solution substitute delivered corresponded to the upward deflection of the MX-hydrogel diaphragm. When the power was removed, the MX-hydrogel membrane

deflected downward due to the decreased pressure caused by the electrolysis bubble recombination [46]. As shown in figure 6(d), with a 2.5 mW driving power as an example, the MX-hydrogel's $\Delta R/R$ tracks well with the displacement, and a maximum $\Delta R/R$ of 2.12% was achieved at a displacement of 322 μm. In other words, the volume of the drug delivered can be well calculated by the MX-hydrogel based strain output $\Delta R/R$ for dosage monitoring. This example application again validates our synthesized MX-hydrogel to be applied in liquid.

4. Conclusion

This paper presents a conductive MX-hydrogel fabricated through a new low-cost cyclic freezing and thawing processes. Excellent mechanical performance has been achieved thanks to the solid interactions between PVA and PVP chains. With the addition of MXene nanoparticles, the hydrogel's GF increases by 61% compared to that of pure hydrogel. Particularly, we performed a thorough study on the effects of water evaporation of the MX-hydrogel. The results reveal that the MX-hydrogel resistance increases with water evaporation due to blocked conductive paths. In liquid, for temperature up to 40 °C, the MX-hydrogel resistance drops by about 0.6 KΩ for every 10 °C of temperature increase. In the paper, we observed that, after soaking a dried sample, its MX-hydrogel's electro-mechanical performance (GF) degrades by 42% due to the inner structure change during the drying or water evaporation process. Finally, the MX-hydrogel diaphragm is used as a dosage sensor which is not far away from the practical application, its deformation provides an actuation for driving the drug solution, and the sensor can output a $\Delta R/R$ that corresponds with the displacement of the MX-hydrogel diaphragm. In the experiment, the $\Delta R/R$ linearly increased to 2.12% with an increased displacement of up to 322 μm, reflecting the MX-hydrogel's ability to monitor the volume of the drug being delivered.

Data availability statement

All data that support the findings of this study are included within the article (and any supplementary files).

Conflict of interest

The authors declare no competing financial interest.

ORCID iDs

Ying Yi ● https://orcid.org/0000-0003-1692-6118
Mu Chiao ● https://orcid.org/0000-0002-9128-3290
Khaled A Mahmoud ● https://orcid.org/0000-0003-1246-4067
Bo Wang ● https://orcid.org/0000-0002-9359-4869

References

[1] Liao X, Wang W, Wang L, Jin H, Shu L, Xu X and Zheng Y 2021 A highly stretchable and deformation-insensitive bionic electronic exteroceptive neural sensor for human-machine interfaces *Nano Energy* **80** 105548

[2] Liao X Q, Song W T, Zhang X, Yan C Q, Li T L, Ren H L, Liu C Z, Wang Y and Zheng Y J 2020 A bioinspired analogous nerve towards artificial intelligence *Nat. Commun.* **11** 1–9

[3] Liao X, Wang W, Wang L, Tang K and Zheng Y 2018 Controllably enhancing stretchability of highly sensitive fiber-based strain sensors for intelligent monitoring *ACS Appl. Mater. Interfaces* **11** 2431–40

[4] Liao X Q, Song W T, Zhang X, Jin H, Liu S Y, Wang Y T, Yew Thean A V and Zheng Y 2021 An artificial peripheral neural system based on highly stretchable and integrated multifunctional sensors *Adv. Funct. Mater.* **31** 2101107

[5] Kim J-H, Kim S-R, Kil H-J, Kim Y-C and Park J-W 2018 Highly conformable, transparent electrodes for epidermal electronics *Nano Lett.* **18** 4531–40

[6] Lin L, Wang L, Li B, Luo J, Huang X, Gao Q, Xue H and Gao J 2020 Dual conductive network enabled superhydrophobic and high performance strain sensors with outstanding electro-thermal performance and extremely high gauge factors *Chem. Eng. J.* **385** 123391

[7] Ying W B *et al* 2020 Waterproof, highly tough, and fast self-healing polyurethane for durable electronic skin *ACS Appl. Mater. Interfaces* **12** 11072–83

[8] Zhang D, Xu S, Zhao X, Qian W, Bowen C R and Yang Y 2020 Wireless monitoring of small strains in intelligent robots via a joule heating effect in stretchable graphene–polymer nanocomposites *Adv. Funct. Mater.* **30** 1910809

[9] Sun X, Yao F and Li J 2020 Nanocomposite hydrogel-based strain and pressure sensors: a review *J. Mater. Chem.* A **8** 18605–23

[10] Yi Y, Chiao M, Mahmoud K A, Wu L and Wang B 2022 Preparation and characterization of PVA/PVP conductive hydrogels formed by freeze–thaw processes as a promising material for sensor applications *J. Mater. Sci.* **57** 8029–38

[11] Li S, Cong Y and Fu J 2021 Tissue adhesive hydrogel bioelectronics *J. Mater. Chem.* B **9** 4423–43

[12] Sarkar B, Li X, Quenneville E, Carignan L-P, Wu K and Cicoira F 2021 Lightweight and flexible conducting polymer sponges and hydrogels for electromagnetic interference shielding *J. Mater. Chem.* C **9** 16558–65

[13] He S *et al* 2021 Non-swelling and anti-fouling MXene nanocomposite hydrogels for underwater strain sensing *Adv. Mater. Technol.* **7** 2101343

[14] Ren J, Liu Y, Wang Z, Chen S, Ma Y, Wei H and Lü S 2022 An anti-swellable hydrogel strain sensor for underwater motion detection *Adv. Funct. Mater.* **32** 2107404

[15] Naficy S, Razal J M, Spinks G M, Wallace G G and Whitten P G 2012 Electrically conductive, tough hydrogels with pH sensitivity *Chem. Mater.* **24** 3425–33

[16] Liu X, Zhang Q, Duan L and Gao G 2019 Bioinspired nucleobase-driven nonswellable adhesive and tough gel with excellent underwater adhesion *ACS Appl. Mater. Interfaces* **11** 6644–51

[17] Li F, Zhang G, Wang Z, Jiang H, Feng X, Yan S, Zhang L, Li H, Zhao T and Liu M 2019 Bioinspired nonswellable ultrastrong nanocomposite hydrogels with long-term underwater superoleophobic behavior *Chem. Eng. J.* **375** 122047

[18] Zheng Q, Jin Y, Liu Z, Ouyang H, Li H, Shi B, Jiang W, Zhang H, Li Z and Wang Z L 2016 Robust multilayered encapsulation for high-performance triboelectric nanogenerator in harsh environment *ACS Appl. Mater. Interfaces* **8** 26697–703

[19] Wang Z, Liu Y, Wang Z, Huang X and Huang W 2021 Hydrogel-based composites: unlimited platforms for biosensors and diagnostics *View* **2** 20200165

[20] Rathod S G, Bhajantri R F, Ravindrachary V, Sheela T, Pujari P K, Naik J and Poojary B 2015 Pressure sensitive dielectric properties of TiO_2 doped PVA/CN-Li nanocomposite *J. Polym. Res.* **22** 1–14

[21] Cai G, Wang J, Qian K, Chen J, Li S and Lee P S 2017 Extremely stretchable strain sensors based on conductive self-healing dynamic cross-links hydrogels for human-motion detection *Adv. Sci.* **4** 1600190

[22] Naguib M, Kurtoglu M, Presser V, Lu J, Niu J, Heon M, Hultman L, Gogotsi Y and Barsoum M W 2011 Two-dimensional nanocrystals produced by exfoliation of Ti_3AlC_2 *Adv. Mater.* **23** 4248–53

[23] Lukatskaya M R, Mashtalir O, Ren C E, Dall'Agnese Y, Rozier P, Taberna P L, Naguib M, Simon P, Barsoum M W and Gogotsi Y 2013 Cation intercalation and high volumetric capacitance of two-dimensional titanium carbide *Science* **341** 1502–5

[24] Ghidiu M, Lukatskaya M R, Zhao M Q, Gogotsi Y and Barsoum M W 2014 Conductive two-dimensional titanium carbide 'clay' with high volumetric capacitance *Nature* **516** 78–81

[25] Pei Y, Zhang X, Hui Z, Zhou J, Huang X, Sun G and Huang W 2021 $Ti_3C_2T_X$ MXene for sensing applications: recent progress, design principles, and future perspectives *ACS Nano* **15** 3996–4017

[26] Zhu Y, Liu J, Guo T, Wang J J, Tang X and Nicolosi V 2021 Multifunctional $Ti_3C_2T_x$ MXene composite hydrogels with strain sensitivity toward absorption-dominated electromagnetic-interference shielding *ACS Nano* **15** 1465–74

[27] Anasori B, Lukatskaya M R and Gogotsi Y 2017 2D metal carbides and nitrides (MXenes) for energy storage *Nat. Rev. Mater.* **2** 1–17

[28] Cai Y, Shen J, Ge G, Zhang Y, Jin W, Huang W, Shao J, Yang J and Dong X 2018 Stretchable $Ti_3C_2T_X$ MXene/carbon nanotube composite based strain sensor with ultrahigh sensitivity and tunable sensing range *ACS Nano* **12** 56–62

[29] Yue Y *et al* 2018 3D hybrid porous MXene-sponge network and its application in piezoresistive sensor *Nano Energy* **50** 79–87

[30] Lu Y, Qu X, Zhao W, Ren Y, Si W, Wang W, Wang Q, Huang W and Dong X 2020 Highly stretchable, elastic, and sensitive MXene-based hydrogel for flexible strain and pressure sensors *Research* **2020** 1–13

[31] Wang P, Li G, Liu J, Hou Z, Meng C, Guo S, Liu C and Fan S 2021 Tailorable capacitive tactile sensor based on stretchable and dissolvable porous silver nanowire/ polyvinyl alcohol nanocomposite hydrogel for wearable human motion detection *Adv. Mater. Interfaces* **8** 2100998

[32] Ben Doudou B, Vivet A, Chen J, Laachachi A, Falher T and Poilâne C 2014 Hybrid carbon nanotube—silica/polyvinyl alcohol nanocomposites films: preparation and characterisation *J. Polym. Res.* **21** 1–9

[33] Rajesh K, Crasta V, Rithin Kumar N, Shetty G and Rekha P 2019 Structural, optical, mechanical and dielectric properties of titanium dioxide doped PVA/PVP nanocomposite *J. Polym. Res.* **26** 1–10

[34] Chen Y-N, Peng L, Liu T, Wang Y, Shi S and Wang H 2016 Poly (vinyl alcohol)–tannic acid hydrogels with excellent mechanical properties and shape memory behaviors *ACS Appl. Mater. Interfaces* **8** 27199–206

[35] Chen K, Zhang D, Yang X, Cui X, Zhang X and Wang Q 2016 Research on torsional friction behavior and fluid load support of PVA/HA composite hydrogel *J. Mech. Behav. Biomed. Mater.* **62** 182–94

[36] Chen K, Liu J, Yang X and Zhang D 2017 Preparation, optimization and property of PVA-HA/PAA composite hydrogel *Mater. Sci. Eng.* C **78** 520–9

[37] Rasool K, Mahmoud K A, Johnson D J, Helal M, Gogotsi Y and Gogotsi Y 2017 Efficient antibacterial membrane based on two-dimensional $Ti_3C_2T_x$ (MXene) nanosheets *Sci. Rep.* **7** 1598

[38] Liu Y-J, Fu L-H, Liu S, Meng L-Y, Li Y-Y and Ma M-G 2016 Synthetic self-assembled homogeneous network hydrogels with high mechanical and recoverable properties for tissue replacement *J. Mater. Chem.* B **4** 4847–54

[39] Choudhary S and Sengwa R 2018 ZnO nanoparticles dispersed PVA–PVP blend matrix based high performance flexible nanodielectrics for multifunctional microelectronic devices *Curr. Appl. Phys.* **18** 1041–58

[40] Hodge R, Edward G H and Simon G P 1996 Water absorption and states of water in semicrystalline poly (vinyl alcohol) films *Polymer* **37** 1371–6

[41] Wei Y *et al* 2020 MXene-based conductive organohydrogels with long-term environmental stability and multifunctionality *Adv. Funct. Mater.* **30** 2005135

[42] Qi C, Dong Z, Huang Y, Xu J and Lei C 2022 Tough, anti-swelling supramolecular hydrogels mediated by surfactant–polymer interactions for underwater sensors *ACS Appl. Mater. Interfaces* **14** 30385–97

[43] Yi Y, Chiao M and Wang B 2021 An electrochemically actuated drug delivery device with *in-situ* dosage sensing *Smart Mater. Struct.* **30** 055003

[44] Yi Y, Buttner U and Foulds I G 2015 A cyclically actuated electrolytic drug delivery device *Lab Chip* **15** 3540–8

[45] Yi Y, Huang R and Li C 2019 Flexible substrate-based thermo-responsive valve applied in electromagnetically powered drug delivery system *J. Mater. Sci.* **54** 3392–402

[46] Yi Y, Buttner U, Carreno A A, Conchouso D and Foulds I G 2015 A pulsed mode electrolytic drug delivery device *J. Micromech. Microeng.* **25** 105011